VERSITA

OPTO-ELECTRONICS REVIEW **19**(3), 327–332

DOI: 10.2478/s11772-011-0029-z

Nanostructuring of thin Au films by means of short UV laser pulses

K. GROCHOWSKA*[1], N. NEDYALKOV[2], P. ATANASOV[2], and G. ŚLIWIŃSKI[1]

[1]The Szewalski Institute, Polish Academy of Sciences, 14 Fiszera Str., 80-231 Gdańsk, Poland
[2]Institute of Electronics, Bulgarian Academy of Sciences, 72 Tzarigradsko Shousse, 1784 Sofia, Bulgaria

The particle size distribution, morphology and optical properties of the Au nanoparticle (NP) structures for surface enhanced Raman signal (SERS) application are investigated in dependence on their preparation conditions. The structures are produced from relatively thin Au films (10–20 nm) sputtered on fused silica glass substrate and irradiated with several pulses (6 ns) of laser radiation at 266 nm and at fluencies in the range of 160–412 mJ/cm^2. The SEM inspection reveals nearly homogeneously distributed, spherical gold particles. Their initial size distribution of the range of 20–60 nm broadens towards larger particle diameters with prolonged irradiation. This is accompanied by an increase in the uncovered surface of the glass substrate and no particle removal is observed. In the absorption profiles of the nanostructures, the broad peak centred at 546 nm is ascribed to resonant absorption of surface plasmons (SPR). The peak position, halfwidth and intensity depend on the shape, size and size distribution of the nanostructured particles in agreement with literature. From peak intensities of the Raman spectra recorded for Rhodamine 6G in the range of 300–1800 cm^{-1}, the relative signal enhancement by factor between 20 and 603 for individual peaks is estimated. The results confirm that the obtained structures can be applied for SERS measurements and sensing.

Keywords: thin Au films, nanostructuring, Au nanoparticles, surface enhanced Raman signal (SERS).

1. Introduction

Noble metal nanostructures are characterized by large optical enhancements such as strong scattering and absorption of light. The enhancements originate from resonant oscillations of the free electrons on the particles surface under irradiation by light. This effect is known as surface plasmon resonance (SPR) and depends on the particle size and shape, and on the size and spatial distributions of the particles. The absorption spectrum of such nanostructures reveals contributions depending on the dielectric properties of the noble metal and of the surrounding (substrate or matrix) as well [1,2].

Among the possible metals investigated for the use in surface enhanced Raman spectroscopy (SERS), the noble metal nanoparticle structures of Au and Ag are preferred substrates. This is due to such advantages as the broad plasmon resonance in the UV-visible-near infrared region, high stability of the structures, and reliable preparation techniques [3–5]. The lithographic ones by means of electron and ion beams, electrospraying, and direct laser 2D and 3D structuring belong to the well proven [6,7]. For silver, the nanoparticle patterning by the pulsed-laser ablation of a silver target and deposition on a glass surface both performed in water is reported and then found to be a highly effective surface-enhanced Raman scattering substrate [8,9]. Recently, the femtosecond laser nanostructuring of SERS substrates on silicon basis has been reported [10].

The nanostructuring of thin Ag films on glass substrates by means of nanosecond UV laser pulses is originally proposed by Henley *et al.* [11]. This technique makes use of the photothermally induced fragmentation of the metal film into nanodroplets which results from poor wetting of the glass substrate by the liquid metal.

In our previous work, the semi-regular, closely packed NP structures were obtained by pulsed laser irradiation at 308 nm of the Au films of a thickness in the range of 60–200 nm [12]. The near field properties of nanostructured thin gold and silver films on glass substrate were investigated theoretically by means of finite difference time domain (FDTD) simulation at parameters corresponding to practical applications [13]. The experimental conditions ensuring thin film modifications which result in spatial characteristics close to uniform were defined. For the obtained nanostructures, the SERS effect was measured. The enhancement of the Raman signal was explained by the electric field distribution and the optical near-field enhancement in the vicinity of produced nanostructures.

In this work we extend the range of experimental conditions of the NPs production by the UV laser melting of noble metal thin films. Instead of the pulsed laser deposition (PLD) technique, the discharge sputtering is used for the thin film preparation and then the structuring of relatively thin films of the thickness not considered yet, i.e., in the

*e-mail: kgrochowska@imp.gda.pl

range of 10-20 nm is investigated. Moreover, laser radiation of shorter UV wavelength and pulsewidth compared to previous experiments, are applied.

2. Experimental

Thin Au films were produced from bulk material (Sigma Aldrich, 99.99% purity) by the discharge sputtering at ambient temperature and a pressure of 4×10^{-2} hPa. Films of a thickness of 10, 15, and 20 nm were sputtered on the glass substrate at a growth rate of 7.5 nm/min measured by the microbalance. The substrate was prepared from the squared (1×1 cm^2) microscope glass slides sonically cleaned in acetone bath. The irradiation of the films for production of the NP structures was performed in vacuum at a pressure of 2×10^{-6} hPa. Samples were irradiated by the pulsed Nd:YAG laser (Quantel B) operated at 266 nm with pulse duration of 6 nm and pulse frequency of 2 Hz. Up to 15 pulses were applied per sample at fixed laser fluencies of 160, 310, and 412 mJ/cm^2 obtained by variation of the laser spot dimension. This was realized by adjusting the lens telescope placed in the laser beam path. The SEM inspection of the samples was performed by means of the scanning electron microscope EVO-40 (Zeiss). For absorbance measurements of the Au NP structures, the spectrophotometer UV 1240 (SHIMADZU) was applied. The SERS measurements were carried out after a droplet of the 0.09 M solution of Rodamine 6G in ethanol was applied on the processed surface of each investigated sample and then dried. The Raman spectra were acquired by means of the InVia confocal instrument (Renishaw) equipped with a 785-nm laser for sample excitation. The laser was operated at the power substantially reduced up to 0.05% of the maximal value. Spectra were collected at the microscope magnification of 50x, and for each spectrum at least 5 scans were accumulated.

3. Results and discussion

The thin film samples deposited by discharge sputtering under above mentioned conditions reveal minimal surface roughness and no surface cracks or other defects. This assures the initial parameters for the structuring similar to these applied in our previous experiments and is found to be of key importance for production of NPs homogeneously distributed over the substrate surface. The fluence values of 160–412 mJ/cm^2 applied during laser irradiation of the 10-nm thick Au films on glass result in the nanostructured samples shown in Fig. 1. The obtained structures typically covered an area of about 1.5 mm in dia. The nearly homogeneous distribution of the particles population which are spherical in shape and differ in diameter is characteristic for all investigated structures, and this observation is consistent with our previous work [12,13]. Depending on the pulse number applied, the particle number per unit area decreases with prolonged irradiation at fixed laser fluence of 412 mJ/cm^2 which indicates on their stepwise spatial rearrangement on the substrate surface, see Figs. 1(a)–(c). Instantaneously, particles of larger diameter appear due to remelting and coalescence of the smaller ones what leads to broadening of the particle size distribution. This conclusion is supported by the comparison of structures produced with the same irradiation pulse number and different fluencies of 412 and 160 mJ/cm^2, see Figs. 1(c) and 1(d). It shows a higher number of particles on the substrate surface for the case of lower fluence applied and indicates again on strong dependence of the nanostructures on irradiation parameters and the total dose applied.

The observed surface morphology is confirmed by the numerical data on particle size distributions. Such data can be extracted from SEM images and values obtained from photographs of Fig. 1(a)–(c) processed by a commercial graphics software are summarized in Fig. 2. Irradiating at low dose, i.e., with 5 pulses results in a relatively narrow size distribution of NPs in the range of 20–80 nm with prevailing number of small ones of diameter between 20 and 40 nm. After application of the next 5 pulses, the number of smallest particles decreases markedly and the maximum of the NP size distribution shifts towards larger diameters of ~80 nm. The distribution flattens and also the total particle number decreases substantially after further irradiation (15 pulses). The effect results from lower viscosity of the liquid droplets and their higher mobility on the substrate under such irradiation conditions which lead to coalescence into bigger particles, and this observation is in agreement with our results reported previously [12].

It is worth to mention, that beside mentioned irradiation parameters, the intensity distribution of the laser beam play a crucial role in the production of homogeneous structures of small size NPs. An example of the Au film locally damaged due to hot spot on the surface irradiated by laser is shown in Fig. 3. This unwanted side effect results in a clear break of the thin film into large, irregularly shaped metal islands characterized by sizes of tens of micrometers, Fig. 3(a). Singular particles with sizes up to few hundreds of nanometers are formed at the edges of these islands. Magnified view of such an edge reveals also a small number of rarely distributed, much smaller nanoparticles, Fig. 3(b). The final result of the local, intensity hot spot is similar to that observed for samples irradiated at fluencies above a certain upper limit. It results in decomposition of the thin film into particles with a flat and wide size distribution with the maximal particle diameter even up to about 500 nm.

The expected enhancement of optical parameters of the Au NP samples originates from large increase in the light scattering and also absorption in the UV and visible range which both result from nanostructuring of the film surface. The spectral profiles of absorption of the nanostructures obtained from gold films of original thickness of 10 nm are shown in Fig. 4 and confirm conclusion drawn from their structures observed in SEM images. In the non-corrected spectra “a”, “b”, and “c”, the sum of two main contributions originating from the nanostructured gold particles and the glass substrate can be identified in agreement with literature data [2,14,15]. The broad peak centred around 546 nm of

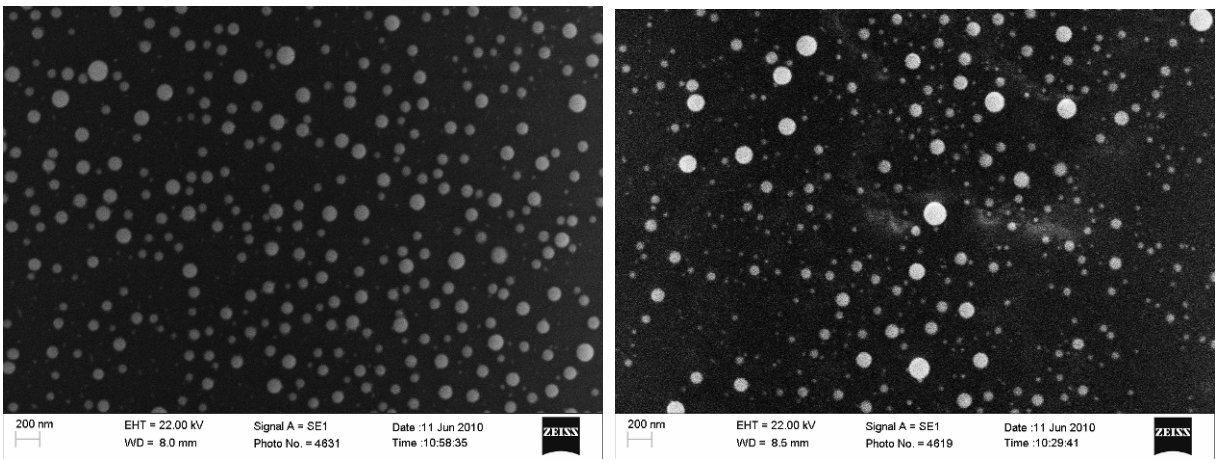

Fig. 1. SEM images of Au nanoparticles obtained from films of the thickness of d ~10 nm, irradiated with 5 (a), 10 (b), and 15 (c) laser pulses at 266 nm and fixed fluence of 412 mJ/cm^2, and with 15 pulses at 160 mJ/cm^2 (d).

the profile close to Lorenzian curve corresponds to the resonant absorption of surface plasmons and defines the strength of the SPR effect which is of importance for SERS applications. This peak reveals a red shift, relative to the resonance position of a single Au molecule [2]. The position of the SPR peak maximum can be controlled by varying the shape and size of the nanoparticles.

The spectral width and height of this peak depends on the size, quantity and shape of particles. The size dependence is confirmed experimentally also for the short dephasing time of 9–15 fs corresponding to the SPR halfwidth [16]. The explanation of the size dependency is possible by the Drude theory of free electron [14]. A broad spectral profile of plasmons is due to particles which are small compared to the electron mean free path and scatter strongly electrons from a surface. The scattering on large particles is substantially weaker and results in the narrower absorption profiles of higher peak intensities. The spectral halfwidth (fwhm) of plasmon peaks in Fig. 4 fitted with Lorenz curve decreases with prolonged irradiation from 94.3 to 79.6 and to 77.4 nm for curves "a", "b", and "c", respectively. It indicates on increasing contribution of larger particles and is consistent with theory, whereas the nearly unchanged peak maxima confirm, that the total number of absorbing centres remains constant independently of the size redistribution. This means that no particle removal from the surface takes place during prolonged irradiation. Moreover, the observed

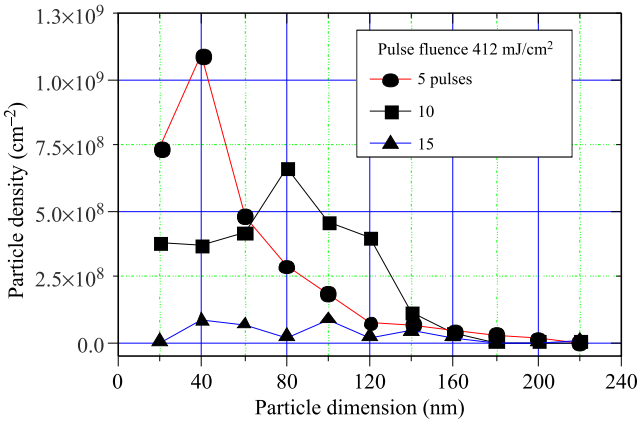

Fig. 2. Size distributions of Au nanoparticles irradiated at fluence of 412 mJ/cm^2; data points: circles, squares, and triangles correspond to SEM images shown in Figs. 1(a)–(c), respectively.

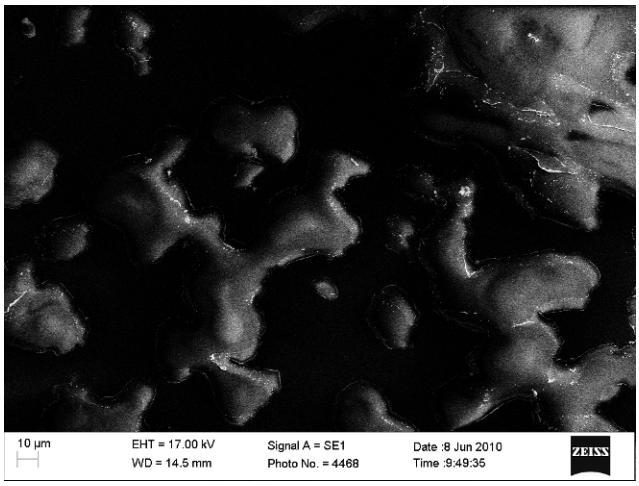

(a)

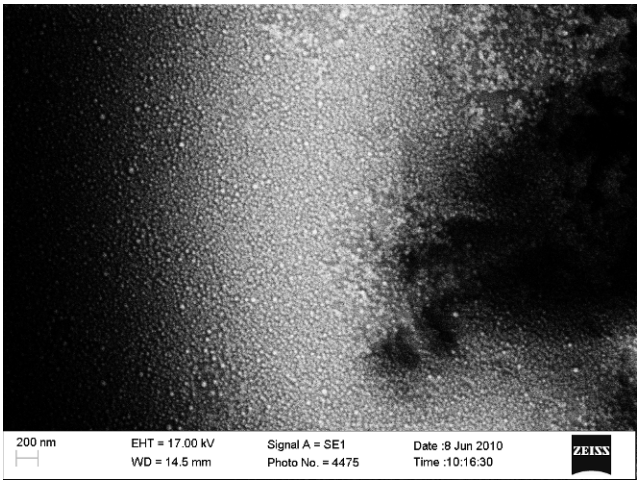

(b)

Fig. 3. Local decomposition of 20-nm thick Au film irradiated at laser fluence of 412 mJ/cm^2 with 5 pulses (a), and 10 pulses (b); in (b) the edge of an irregular Au island on glass is shown.

linewidth and intensity are in agreement with the slight redshifts of the peak maxima – see inset of Fig. 4, which can also be explained by the shift in the particle size distribution with growing number of larger particles.

The role of particle size originates mostly from the size-dependent dielectric function $\varepsilon(\omega) = \varepsilon_1(\omega) - i\varepsilon_2(\omega)$ of the Au core electrons, which results from the partial screening at the surface region and changing the electronic structures at the interband transitions. The resulting plasmon peak is offset by the large, near-linear interband term of the real and imaginary components $\varepsilon_1(\omega)$ and $\varepsilon_2(\omega)$ of the susceptibility whereas in case of $\varepsilon_2(\omega)$, the free electron contribution becomes dominant in the above visible region. The offset is shown schematically by the solid line in Fig. 4. The intensity increase in the wings of profiles "b" and "c" can be explained by the growing contribution of the glass absorption due to stepwise uncovering of the substrate.

The profile and position of the plasmon absorption peak can be derived by using the Maxwell-Garnett approach with

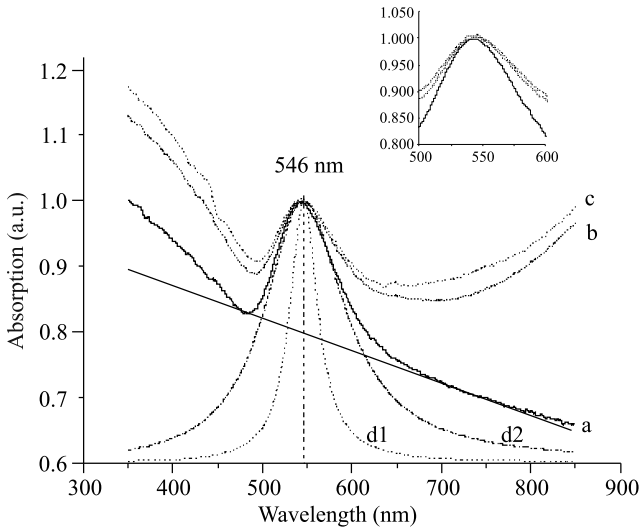

Fig. 4. Absorption spectra of the Au nanoparticle structures on glass substrate; spectral profiles "a", "b", and "c" correspond to structures shown in Figs. 1(a), 1(b), and 1(c), respectively; inset shows slight redshifts of the "b" and "c" peak centres relative to "a"; normalized spectra ($d1$) and ($d2$) are calculated for particle dimension of 20 nm and 4 nm.

the assumed Lorentz "cavity" field inside and outside particles [4] or directly from the Mie absorption and scattering theory [14], both leading finally to the relation

$$\alpha = 18\pi R^3 NV \frac{1}{\lambda} \frac{\varepsilon_2}{\lambda(\varepsilon_1 + 2n^2)^2 + \varepsilon_2^2}, \qquad (1)$$

with

$$NV = \Phi \frac{\rho_{Au}}{\rho_S}, \qquad (2)$$

where Φ is the volume fraction of gold in the structure, N is the number of particles of the radius R per unit volume, V is the volume of a single particle, n is the refraction index of the structure, and ρ_{Au}, ρ_S are the density of Au (19.3 g/cm^{-3}) and its concentration in the structure (4.75×10^{-4} g/cm^{-3}). The values of $\varepsilon_1 = 10 - 58\lambda^2$ and $\varepsilon_2 = 0.1 + 3.4(l_0/R+1)\lambda^3$, with wavelength in µm as in Eqs. (1) and (2), are justified by the measurements of Theye [17] and also by Vosburgh and Doremus [14]. They take into account the mentioned free-electron component of ε_1 extrapolated at $\lambda > 0.48$ µm, and the correction of ε_2 due to particle dimension relative to the mean free path of electrons in the bulk l_0. The normalized spectral profiles calculated for l_0 = 20 nm and for the particle dimension of 20 nm and 4 nm are shown as the spectra $d1$ and $d2$ in Fig. 4. For the position coincidence of calculated peaks with the measured ones, an arbitrary redshift is applied by assuming slightly elevated value of $n = 1.9$ in the calculus. This value has been estimated from data reported for Au nanoparticles characterized by an absorption band centred at 546 nm [19]. The originally calculated spectrum $d1$ (fwhm = 38 nm) broadens to the shape of spectrum $d2$ (fwhm = 107 nm) with the particle dimension decreasing from 20 to 4 nm. On the other hand, the observed

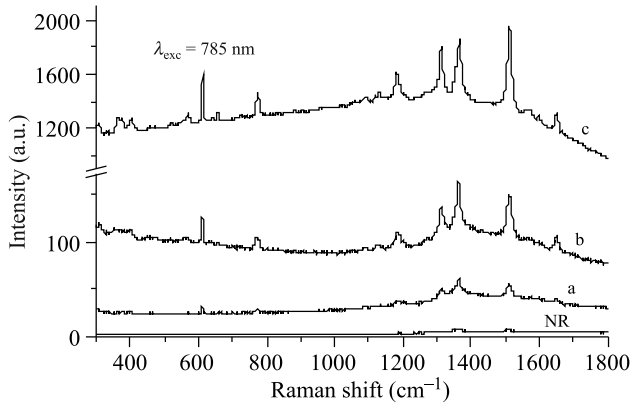

Fig. 5. Comparison between the Raman spectra of R6G deposited on: glass – NR (after Ref. 12), (a) – Au non-structured film, and (b), (c) – gold nanoparticle structures shown in Figs. 1(d) and 1(a), respectively; samples excited at λ = 785 nm.

discrepancies indicate that in order to explain the case of small volume fractions (~10^{-4}) accompanied by certain size distribution of the particles both effects should be taken into account by introducing additional correction factors in the calculation.

For measurement of the SER signal, the spectra of samples covered with dried film of the RG6 solution are recorded under mild excitation at 785 nm which should provide efficient near field enhancement at strong Raman signal, in agreement with numerical simulation and literature data [13,18,20]. Figure 5 shows non-corrected Raman spectra of R6G deposited on glass (NR), on the 10-nm thick Au film on glass "a" and on the nanostructured gold substrates presented in Figs. 1(a) and (d).

Compared to the vanishingly weak, luminescence-free (NR) signal, the spectral structure "a" shows slight enhancement of peaks typical for the R6G Raman spectrum which are centered at 610, 774, 1180, 1312, 1366, and 1512 cm^{-1}. This somehow surprising result can be explained by the structure of the sputtered gold film, which reveals the EM-field enhancement at interstitial sites prior modification by laser pulses. This is characteristic of closely packed structure which in case of very small particles (size less than 0.5 nm) is accompanied by substantially broadened absorption band discussed in the literature [2,14]. Due to the elevated background of spectra "a", "b", and "c", the parasitic noise contribution from remnants of the Au film and from glass substrate cannot be excluded and consideration of the quantitative signal enhancement can only be estimated. Nevertheless, direct comparison of the peak intensities of spectrum (NR) with these of "b" and "c" in the range of 600–1550 cm^{-1} shows relative enhancement of the Raman signal by a factor varying between 20–48 and 239–603 for individual peaks of spectra "b" and "c", respectively. This result is more than satisfactory because the properties of nanostructure discussed here in part only match these of large SERS ensured in interstices between nanoparticles smaller than reported here and with distances of less than 5 nm, where the intensity can build up by several orders of magnitude [12].

4. Conclusions

For the preparation of SERS active surfaces, the thin (10–20 nm) Au films sputtered on glass represent an interesting alternative to much thicker substrates prepared by the PLD technique. Nearly homogeneous nanostructures of spherical gold particles and narrow particle size distribution can be prepared by selection of certain parameters of the pulsed UV laser irradiation at relatively high laser fluencies. In order to minimize negative side effects, such as the local structure inhomogeneity, the care should be taken to avoid hot spots in the intensity distribution of the laser beam during sample processing.

The absorption profiles of the nanostructured Au NP substrates show dependency on their preparation conditions and on the shape, size and size distribution of the produced particles, in agreement with literature. The Raman spectra clearly reveal the relative surface enhancement of the signal by almost three orders of magnitude and confirm that the obtained structures can be applied for SERS measurements and sensing.

Larger enhancement of the Raman signal is expected for smaller particles forming closely packed structures of controlled geometry and work on this topic aimed on SERS applications is in progress.

Acknowledgements

The authors appreciate financial support of the Bulgarian National Science Fund via project DO-02-293, the BAN-PAN Bilateral Project 33/10, and of the project 19/DWI/08 of the Ministry of Science and Higher Education of Poland – MNiSW. The technical assistance of Dr M. Sawczak and Mr A. Sobczyk is gratefully acknowledged.

References

1. U. Kreibig and M. Vollmer, *Optical Properties of Metal Clusters*, Springer, Berlin, 1995.
2. M.M. Alvarez, J.T. Khoury, T.G. Schaaff, M.N. Shafigullin, I. Vezmar, and R.L. Whetten, "Optical absorption spectra of nanocrystal gold molecules", *J. Phys. Chem.* **B101**, 3706–3712 (1997).
3. J. Yao, A.P. Le, S.K. Gray, J.S. Moore, J.A. Rogers, and R.G. Nuzzo, "Functional nanostructured plasmonic materials", *Adv. Mater.* **22**, 1102–1110 (2010).
4. T. Ung, L.M. Liz-Marzan, and P. Mulvaney, "Gold nanoparticle thin films", *Colloid Surface.* **A202**, 119–126 (2002).
5. M.A. Garcia, J. de la Venta, P. Crespo, J. Llopis, P. Penades, A. Fernandez, and A. Hernando, "Surface plasmon resonance of capped Au nanoparticles", *Phys. Rev.* **B72**, 241403R (2005).
6. Y.E. Guan and A.J. Pedraza, "Synthesis of aligned nanoparticles on laser-generated templates", *Nanotechnology* **16**, 1612 (2005).
7. J. Koch, F. Korte, C. Fallnich, A. Ostendorf, and B.N. Chichkov, "Direct-write sub-wavelength structuring with femtosecond laser pulses", *Opt. Eng.* **44**, 051103 (2005).

8. P. Šmejkal, J. Pfleger, B. Vlčková, and O. Dammer, "Laser ablation of silver in aqueous ambient: effect of laser pulse wavelength and energy on efficiency of the process", *J. Phys: Conf. Ser.* **59**, 185–188 (2007).
9. H. Cui, P. Liu, and G.W. Yang, "Noble metal nanoparticle patterning deposition using pulsed-laser deposition in liquid for surface-enhanced Raman scattering", *App. Phys. Lett.* **89**, 153–124 (2006).
10. E. Diebold, N. Mack, S. Doorn, and E. Mazur, "Femtosecond laser-nanostructured substrates for surface-enhanced Raman scattering", *Langmuir* **25**, 1790 (2009).
11. S.J. Henley, J.D. Carey, and S.R. Silva, "Metal nanoparticle production by pulsed laser nanostructuring of thin metal films", *Appl. Surf. Sci.* **253**, 8080 (2007).
12. S.E. Imamova, A. Dikovska, N.N. Nedyalkov, P.A. Atanasov, M. Sawczak, R. Jendrzejewski, G. Śliwiński, and M. Obara, "Laser nanostructuring of thin Au films for application in surface enhanced Raman spectroscopy", *J. Optoelectron. Adv. M.* **12**, 500–504 (2010).
13. N.N. Nedyalkov, S.E. Imamova, P.A. Atanasov, and M. Obara, "Near field localization mediated by a single gold nanoparticle embedded in transparent matrix: Application for surface modification", *Appl. Surf. Sci.* **255**, 5125–5129 (2009).
14. J. Vosburgh and R.H. Doremus, "Optical absorption spectra of gold nano-clusters in potassium borosilicate glass", *J. Non-Cryst. Solids* **349**, 309–314 (2004).
15. E.N. Boulos, L.B. Glebov, and T.V. Smirnova, "Absorption of iron and water in the Na_2O-CaO-MgO-SiO_2 glasses. I. Separation of ferrous and hydroxyl spectra in the near IR region", *J. Non-Cryst. Solids* **221**, 213–221 (1997).
16. T. Ziegler, C. Hendrich, F. Hubenthal, T. Vartanyan, and F. Trager, "Dephasing times of surface plasmon excitation in Au nanoparticles determined by persistent spectral hole burning", *Chem. Phys. Lett*. **386**, 319–324 (2004).
17. M.L. Theye, "Investigation of the optical properties of Au by means of thin semitransparent films", *Phys. Rev.* **B2**, 3060–3078 (1970).
18. G. Li, H. Li, Y. Mo, X. Huang, and L. Chen, "Surface enhanced resonance Raman spectroscopy of rhodamine 6G adsorbed on silver electrode in lithium batteries", *Chem. Phys. Lett.* **330**, 249–254 (2000).
19. I.I.S. Lim and C.J. Zhong, "Molecularly-mediated assembly of gold nanoparticles", *Gold Bull.* **40**, 59–66 (2007).
20. M. Michaels, J. Jiang, and L. Brus, "Ag nanocrystal junctions as the site for surface-enhanced Raman scattering of single rhodamine 6G molecules", *J. Phys. Chem.* **B104**, 11965–11971 (2000).

